

# Deterministic generation of maximally discordant mixed states by dissipation

X. X. Li, H. D. Yin,\* D. X. Li, and X. Q. Shao†

Center for Quantum Sciences and School of Physics, Northeast Normal University, Changchun 130024, China and  
Center for Advanced Optoelectronic Functional Materials Research,  
and Key Laboratory for UV Light-Emitting Materials and Technology of Ministry of Education,  
Northeast Normal University, Changchun 130024, China

Entanglement can be considered as a special quantum correlation, but not the only kind. It is allowed to exist non-classical correlations even for a separable quantum system. Here we propose two dissipative schemes for generating a maximally correlated state of two qubits in the absence of quantum entanglement, which was raised by [F. Galve, G. L. Giorgi, and R. Zambrini, *Phys. Rev. A* **83**, 012102 (2011)]. These protocols take full advantages of the interaction between four-level atoms and strongly lossy optical cavities. In the first scenario, we alternatively change the phases of Rabi frequencies of two classical driving fields, while the second proposal introduces a strongly lossy coupled-cavity system. Both schemes can realize all Lindblad terms required by the dissipative dynamics, guaranteeing the maximally quantum dissonant state to be the unique steady state for a certain subspace of system. Moreover, since the target state is a mixed state, the performance of our method is evaluated by the definition of super-fidelity  $G(\rho_1, \rho_2)$ , and the strictly numerical simulations indicate that fidelity outstripping 99% of the quantum dissonant state is achievable with the current cavity quantum electrodynamics parameters.

## I. INTRODUCTION

As one of the most striking features in quantum theory, quantum entanglement is recognized as the essential resource for quantum information processing [1]. For instance, it is widely used in quantum key distribution [2], superdense coding [3], quantum teleportation [4], and quantum computation [5]. Although the best performance of such tasks requires maximally entangled states (Bell states), the decoherence effects due to the environment make the pure entangled state into a statistical mixture and degrade quantum entanglement in reality. For these entangled mixed states, there are more complicated and lesser understood than pure states. Werner state is a typical mixed state defined by a class of two-body quantum mixtures, which is invariant under the unitary transformation [6]. It has been used in the description of noisy quantum channels, such as nonadditivity claims, and in the study of deterministic purification [7].

Quantum discord (QD), a measure of the total quantum correlations, is defined as the difference between the quantum mutual information and the classical correlations at the quantum level [8]. It attempts to quantify all quantum correlations including entanglement. The study of QD has a crucial importance for the full development of new quantum technology because it is more robust than entanglement against the effects of decoherence [9, 10]. Now it has been shown experimentally how to encode quantum information in separable Gaussian states, which introduces an operational protocol to use quantum discord as a resource even in the absence of entanglement [11]. In 2011, Glave *et.al* found some mixed states have greater values of QD than pure states [12], and they identified the family of mixed states which maximize the discord for a given value of the classical correlations. On the basis of

this work, López *et.al* mathematically described a method to produce the maximally correlated states without entanglement [13] and gave an example of unitary dynamic process, which places restrictions on the evolution time of system.

It is well known that the quantum dissipation characterized by a Lindblad generator in Markovian quantum master equations is induced by the weak coupling between quantum systems and environment. Traditionally, it has been considered only having detrimental effects on quantum information processing. Nevertheless, recent studies show that the environment can be used as a resource for quantum computation and entanglement generation [14–29]. In particular, Kastoryano *et.al* [17] discussed the possibility of preparing highly entangled states via the loss of photon from an optical cavity. In Ref. [19], the authors proposed a dissipative scheme to generate a maximally entanglement between two Rydberg atoms, where the spontaneous emissions of atoms play a positive role during the dynamic evolution. And Emanuele *et.al* presented and analyzed a new approach for the generation of atomic spin-squeezed states using the interaction between four-level atoms and a single-mode cavity [30].

Enlightened by the work of Ref. [30], we construct two physical models by taking the environment as a resource to generate the maximally quantum dissonant state. This approach has the following advantages: (i) Compared with the unitary dynamic evolution, the dissipative process is not limited by time. (ii) The initial state is not strictly required by both schemes, and the target state can be successfully prepared as long as the state  $|\Psi^-\rangle = 1/\sqrt{2}(|01\rangle - |10\rangle)$  is not populated initially. (iii) The investigated systems make full use of the cavity decay  $\kappa$  while suppress the spontaneous emission  $\gamma$  of atoms. Therefore, the parameters  $\kappa$  and  $\gamma$  are permitted to have a wide range of values to improve the experimental feasibility.

The remainder of the paper is organized as follows. In Sec. II, we briefly review the properties of maximally correlation states. In Sec. III, we construct one physical model with a pair of four-level atoms trapped in a strongly loss op-

\* yinhd239@nenu.edu.cn

† shaoxq644@nenu.edu.cn

tical cavity. Under the large decay of cavity and alternatively changing the Rabi frequencies of classical fields, we derive an effective master equation and numerically simulate the effects of relevant parameters on the prepared state. In Sec. IV, we introduce another physical model which requires a coupled-cavity with atoms separately trapped in each cavity. In Sec. V and Sec. VI we discuss the potential experimental feasibility and make a brief summary of the work, respectively.

## II. BRIEF REVIEW OF THE MAXIMALLY DISCORDANT MIXED STATES

The states we are interested in are found within the set of separable states. It has been shown that the most nonclassical two-qubit states, i.e., the family with maximal quantum discord versus classical correlations, were formed by mixed states of rank 2 and 3, which are named maximally discordant mixed states (MDMS). The class of states of rank 3 thus defined by [12]

$$\rho = \epsilon|\Phi^+\rangle\langle\Phi^+| + (1-\epsilon)[x|01\rangle\langle 01| + (1-x)|10\rangle\langle 10|], \quad (1)$$

where  $|\Phi^+\rangle = (|00\rangle + |11\rangle)/\sqrt{2}$ .

The definition of quantum correlation is  $I = S(\rho_A) + S(\rho_B) - S(\rho_{AB})$  and the classical correlation is  $C(\rho_{AB}) = \max\{S(\rho_A) - S(\rho_{A|B})\}$ , where  $S(\rho_{A|B})$  is the conditional entropy of  $A$  given a measurement on the system  $B$  while the optimization is over all possible projective measurement on system  $B$ . Refer to Ali-Rau-Alber results of the conditional entropy [31], it is not difficult to find that for  $x = 1/2$  and  $\epsilon = 1/3$  the quantum mutual information is maximized and the classical correlation is minimized. By changing the basis vector of the second qubit, i.e.  $|0\rangle \leftrightarrow |1\rangle$ , we obtain the target state:

$$\rho = \frac{1}{3}(|\Psi^+\rangle\langle\Psi^+| + |00\rangle\langle 00| + |11\rangle\langle 11|), \quad (2)$$

where  $|\Psi^+\rangle = (|01\rangle + |10\rangle)/\sqrt{2}$ .

Using the basis of Bell states  $|\Phi^\pm\rangle = 1/\sqrt{2}(|00\rangle \pm |11\rangle)$ ,  $|\Psi^\pm\rangle = 1/\sqrt{2}(|01\rangle \pm |10\rangle)$  [13], the target state could be rewritten as:

$$\rho = \frac{1}{3}(|\Phi^+\rangle\langle\Phi^+| + |\Phi^-\rangle\langle\Phi^-| + |\Psi^+\rangle\langle\Psi^+|). \quad (3)$$

If we have a system characterized by the following master equation

$$\dot{\rho} = \mathcal{L}_{\gamma_x}(S_x)\rho + \mathcal{L}_{\gamma_{y(z)}}(S_{y(z)})\rho, \quad (4)$$

where  $S_x = (\sigma_x^1 + \sigma_x^2)$ ,  $S_y = (\sigma_y^1 + \sigma_y^2)$ , and  $S_z = (\sigma_z^1 + \sigma_z^2)$  ( $\sigma_{x,y,z}$  are spin operators), the state described by Eq. (3) will be the steady state of this system. However, it is difficult to find a natural system with the above form of the master equation. Thus we consider to design an effective physical model which is equivalent to Eq. (4) under the appropriate approximations, and we will discuss our method detailedly in the next section.

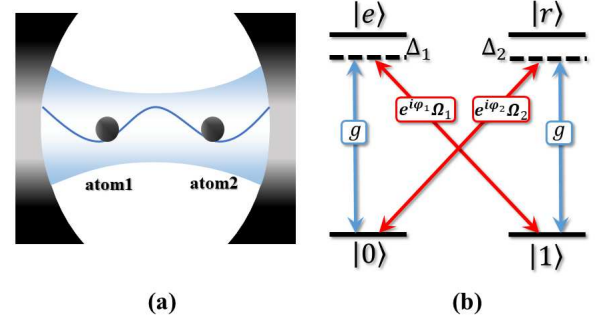


FIG. 1. Schematic view of the system and the configuration of the atoms. (a) The system consists of two atoms collectively interacting with a lossy cavity. (b) Level structure of a four-level atom which is simultaneously driven by two classical fields and coupled to a cavity mode.

## III. TWO FOUR-LEVEL ATOMS IN A LOSSY CAVITY

The central idea of our work can be understood by considering a pair of atoms interacting with a strongly loss optical cavity characterized in Fig. 1. The atoms are simultaneously driven by the laser fields with complex Rabi frequencies  $\Omega_{1(2)}e^{i\varphi_{1(2)}}$  and the quantum field with coupling strength  $g$ . The Hamiltonian under the Schrödinger picture can be written as ( $\hbar = 1$ ):

$$H_s = H_0 + V_s, \quad (5)$$

$$H_0 = \sum_{i=1}^2 \omega_0 |0\rangle_i \langle 0| + \omega_1 |1\rangle_i \langle 1| + \omega_e |e\rangle_i \langle e| + \omega_r |r\rangle_i \langle r| + \nu a^\dagger a, \\ V_s = \sum_{i=1}^2 g(|e\rangle_i \langle 0| + |r\rangle_i \langle 1|)a + \Omega_1 e^{i\varphi_1} |e\rangle_i \langle 1| e^{-i\mu_1 t} + \Omega_2 e^{i\varphi_2} |r\rangle_i \langle 0| e^{-i\mu_2 t} + \text{H.c.},$$

where  $\omega_0$ ,  $\omega_1$ ,  $\omega_e$ , and  $\omega_r$  are the eigenfrequencies of the lower states  $|0\rangle$ ,  $|1\rangle$  and upper states  $|e\rangle$ ,  $|r\rangle$ , respectively, while  $\nu$  and  $\mu_{1(2)}$  are the frequencies of quantum and classical fields.  $a^\dagger$  and  $a$  are the creation and annihilation operators of the optical cavity mode. In addition, the ground states transition is dipole-forbidden. For simplicity, we assume all parameters are real. In the interaction picture, the Hamiltonian of the system reads:

$$H_I = H_1 + H_2, \quad (6)$$

$$H_1 = \sum_{i=1}^2 g a |e\rangle_i \langle 0| e^{i\delta_1 t} + \Omega_1 e^{i\varphi_1} |e\rangle_i \langle 1| e^{i\delta_2 t} + \text{H.c.},$$

$$H_2 = \sum_{i=1}^2 g a |r\rangle_i \langle 1| e^{i\delta_1 t} + \Omega_2 e^{i\varphi_2} |r\rangle_i \langle 0| e^{i\delta_2 t} + \text{H.c.},$$

where  $\delta_{1(2)} = \omega_e - \omega_{0(1)} - \nu(\mu_1)$  and  $\delta'_{1(2)} = \omega_r - \omega_{1(0)} - \nu(\mu_2)$ . We further suppose  $\delta_1 = \delta_2 = \Delta_1$  and  $\delta'_1 = \delta'_2 = \Delta_2$ . Now we consider the process of constructing the collective decay operator  $S_y = \sigma_y^1 + \sigma_y^2$ . Taking  $\Omega_1 e^{i\varphi_1} = -i\Omega_1$ , and  $\Omega_2 e^{i\varphi_2} = i\Omega_2$ , and in the regime of large detuning  $|\Delta_{1(2)}| \gg \{g, \Omega_{1(2)}\}$ , we may safely eliminate the upper states  $|e\rangle$  and  $|r\rangle$ , then the above Hamiltonian reduces to

$$H_{\text{eff}} = H_{\text{eff}}^1 + H_{\text{eff}}^2, \quad (7)$$

where

$$H_{\text{eff}}^1 = G_1 J_- a^\dagger + \text{H.c.} + \sum_{i=1}^2 g_{\text{eff}}^1 a^\dagger a |0\rangle_i \langle 0| + \Omega_{\text{eff}}^1 |1\rangle_i \langle 1|,$$

$$H_{\text{eff}}^2 = G_2 J_+ a^\dagger + \text{H.c.} + \sum_{i=1}^2 g_{\text{eff}}^2 a^\dagger a |1\rangle_i \langle 1| + \Omega_{\text{eff}}^2 |0\rangle_i \langle 0|,$$

where  $G_{1(2)} = g\Omega_{1(2)}/\Delta_{1(2)}$ ,  $g_{\text{eff}}^{1(2)} = -g^2/\Delta_{1(2)}$ , and  $\Omega_{\text{eff}}^{1(2)} = \Omega_{1(2)}^2/\Delta_{1(2)}$ .  $J_- = -i(|1\rangle_1 \langle 0| + |1\rangle_2 \langle 0|)$  and  $J_+ = i(|0\rangle_1 \langle 1| + |0\rangle_2 \langle 1|)$  are the collective ascending and descending operators. If we further assume  $G_1 = G_2 = G$ , i.e.  $\Omega_1/\Delta_1 = \Omega_2/\Delta_2$ , and omit the Stark shifts of the ground states induced by the quantum field and the classical fields, the above Hamiltonian could be simplified as

$$H_{\text{eff}} = G(J_- + J_+)a^\dagger + \text{H.c.} \quad (8)$$

Since the effective system only includes the ground states, the spontaneous emissions of atoms are greatly suppressed, and the master equation could be written as

$$\dot{\rho} = -i[G(J_- + J_+)a^\dagger + G(J_- + J_+)a, \rho] + \frac{\kappa}{2}(2a\rho a^\dagger - a^\dagger a\rho - \rho a^\dagger a). \quad (9)$$

In the limitation of large decay rate  $\kappa \gg G$ , the cavity mode can also be neglected, and we obtain the master equation characterizing the system of atoms as:

$$\dot{\rho} = \Gamma(D[J_-]\rho + D[J_+]\rho) = \mathcal{L}_{\gamma_y}(S_y)\rho, \quad (10)$$

where  $\Gamma = 4G^2/\kappa$  is the collective decay rate of the atoms, and the superoperator  $D$  is defined as  $D[O] = (2O\rho O^\dagger - O^\dagger O\rho - \rho O^\dagger O)/2$ .

Otherwise, if we attempt to construct the collective decay operator  $S_x = \sigma_x^1 + \sigma_x^2$ , we may simply take  $\varphi_1 = \varphi_2 = 0$ , then after a series of similar derivations, the effective master equation reads

$$\dot{\rho} = \Gamma(D[J'_-]\rho + D[J'_+]\rho) = \mathcal{L}_{\gamma_x}(S_x)\rho, \quad (11)$$

where  $J'_+ = |1\rangle_1 \langle 0| + |1\rangle_2 \langle 0|$  and  $J'_- = |0\rangle_1 \langle 1| + |0\rangle_2 \langle 1|$ .

Up to present, we have shown how to generate the collective operators  $S_x$  and  $S_y$  respectively. But the stability of Eq. (3) requires there should be  $\mathcal{L}_{\gamma_x}(S_x)$  and  $\mathcal{L}_{\gamma_y}(S_y)$  in the master equation at the same time. Fortunately, drawing lessons from the spin echoes effect, our model is able to simulate the effective master equation of Eq. (4) apart from a coefficient  $1/2$ , as long as the phases of the classical fields  $\varphi_1$  and  $\varphi_2$

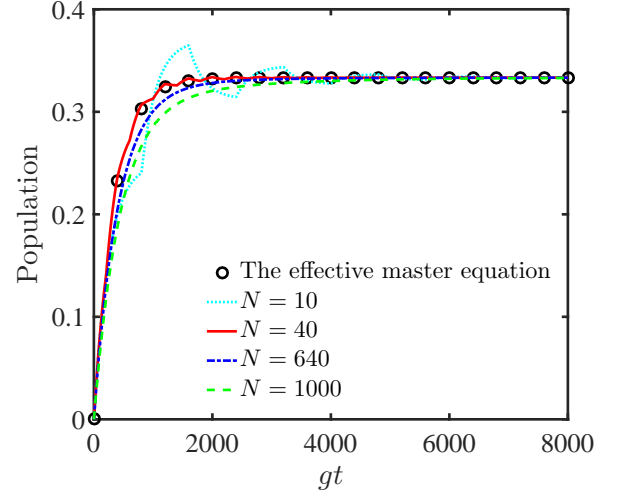


FIG. 2. The populations of  $|\Psi^+\rangle$  as functions of  $gt$  governed by the effective master equation (13) and the master equations with Hamiltonian (6), where  $N$  is the switching number. The initial state is  $\rho_0 = |00\rangle|0\rangle_c$  and we set  $G = 0.01$  and  $\kappa = 80G$ .

are interchanged fast enough. The result is obtained by using the Trotter product formula (see Corollary 5.8 in Chap. III of Ref. [32])

$$\lim_{N \rightarrow \infty} [e^{-\mathcal{L}_{\gamma_x}(S_x)T/2N} e^{-\mathcal{L}_{\gamma_y}(S_y)T/2N}]^N = e^{\frac{1}{2}[\mathcal{L}_{\gamma_x}(S_x) + \mathcal{L}_{\gamma_y}(S_y)]T}, \quad (12)$$

where  $T$  is the total evolution time. Then the effective master equation is

$$\dot{\rho} = \frac{1}{2}[\mathcal{L}_{\gamma_x}(S_x) + \mathcal{L}_{\gamma_y}(S_y)]\rho. \quad (13)$$

Fig. 2 shows the population of  $|\Psi^+\rangle$  under different evolution processes with initial state  $|00\rangle|0\rangle_c$ . The evolution of the effective master equation (13) is shown with empty circles and the other lines are the switching evolution results of the master equation with Hamiltonian (6) together considering the cavity decay  $\kappa$ . The total evolution time is  $gt = 8000$ . Different lines correspond to the results with different switching number  $N$ . With the increasing of  $N$ , line gets nearly to the empty circles. But since the cavity decay is a resource for states generation, the switching number  $N$  has an upper limit keeping the interval time much larger than  $1/\kappa$ , which guarantees the role of  $\kappa$  in each process. And the longer operation time  $1/\Gamma$  determines the minimum value of  $N$  ensuring the interval time far less than  $1/\Gamma$ . Thus we choose  $N = 200$ ,  $gt = 8000$  in the following simulations.

In quantum information theory, distinguishing two quantum states is a fundamental task. One of the main tools used in distinguishability theory is quantum fidelity [33, 34], which is widely used and has been found applications in solving some problems like quantifying entanglement [35, 36], quantum error correction [37], quantum chaos [38] and so on. In order to measure the distance between quantum states including mixed

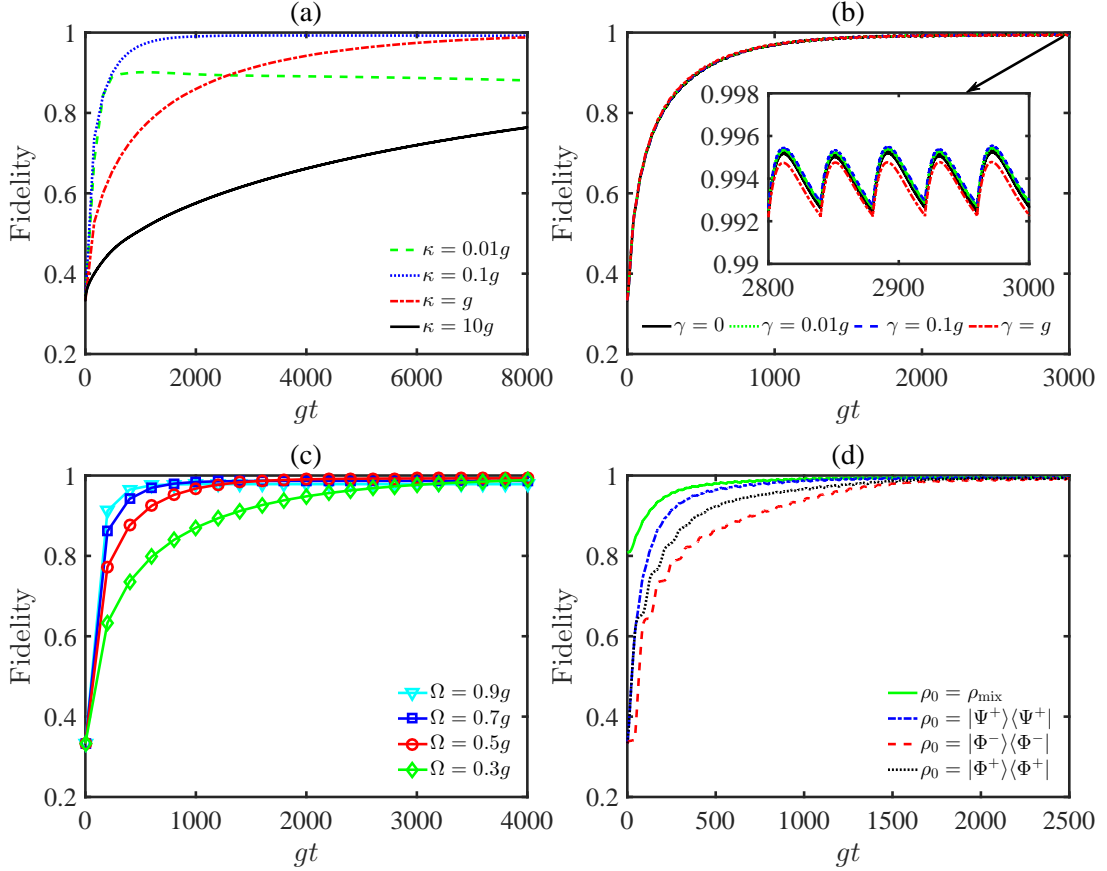


FIG. 3. The target state fidelities as functions of  $gt$  governed by the full master equation and the switching number  $N = 200$ . (a) Time evolutions with different cavity decay rates  $\kappa = (0.01, 0.1, 1, 10)g$ , where we set  $g = 1$ ,  $\Delta_{1,2} = 100g$ , and  $\Omega_{1(2)} = 0.5g$ . (b) Discussion of the effect of atom spontaneous emission rates  $\gamma$  with the same parameters as (a) and  $\kappa = 0.1g$ . The inset shows the enlarge view of the part indicated by the arrow. (c) The effect of Rabi frequencies on the target state with  $\gamma = 0.1g$  and  $\kappa = 0.1g$ . (d) Time evolutions with different initial states, where  $|\Phi^\pm\rangle = 1/\sqrt{2}(|00\rangle|0\rangle_c \pm |11\rangle|0\rangle_c)$ ,  $|\Psi^+\rangle = 1/\sqrt{2}(|01\rangle|0\rangle_c + |10\rangle|0\rangle_c)$ , and  $\rho_{\text{mix}} = (0.1|\Phi^+\rangle\langle\Phi^+| + 0.1|\Phi^-\rangle\langle\Phi^-| + 0.8|\Psi^+\rangle\langle\Psi^+|) \otimes |0\rangle_c\langle 0|$ .

states, we adopt the definition of super-fidelity [39]

$$G(\rho, \sigma) = \text{Tr}[\rho(t)\sigma] + \sqrt{[1 - \text{Tr}\rho(t)^2][1 - \text{Tr}\sigma^2]}, \quad (14)$$

with  $\sigma$  being the density operator of the target state as  $\sigma = 1/3(|\Psi^+\rangle\langle\Psi^+| + |00\rangle\langle 00| + |11\rangle\langle 11|)$ . We initialize the system into state  $|00\rangle|0\rangle_c$  and plot the fidelity of the target-state under the switching evolution of the master equations with full Hamiltonian (6). Figure 3(a), 3(b), and 3(c) respectively discuss the effects of parameters  $\kappa$ ,  $\gamma$ , and  $\Omega$  on the preparation of the target state. Fig. 3(a) shows the fidelity as a function of the cavity decay  $\kappa$  with parameters  $g = 1$ ,  $\Delta_{1,2} = 100g$ , and  $\Omega_{1,2} = 0.5g$ . The increase of  $\kappa$  will prolong the convergence time. It can be explained by Eq. (10). To obtain the target state, the coupling strength  $4G^2/\kappa$  will increase as  $\kappa$  decreasing, which results in a short convergence time. But if  $\kappa$  is too small, it will destroy the condition  $\kappa \gg G$  and fail to generate the target state.

In Fig. 3(b), we take into account the spontaneous emissions of the atoms and plot the evolution of the target state with different  $\gamma$ . Even if  $\gamma$  is extremely large ( $\gamma \sim g$ ), the fidelity is still above 0.99, which demonstrates that our scheme

have favorable resistance to spontaneous emission. The inset picture of Fig. 3(b) is the enlarge view of the part indicated by the arrow. It shows that as  $\gamma = 0 \sim 0.1g$ , the spontaneous emission is a positive factor which successfully enhances the fidelity by dissipating some high-level items to the ground states. But when  $\gamma$  increases to  $g$ , the excessive spontaneous emission becomes negative to our model. In addition, the population keeps oscillating at the final time with small amplitude, and stays around a definite value.

Moreover, the convergence time is related to the intensity of the classical field  $\Omega_{1(2)}$ . Fig. 3(c) displays the evolution curves under different  $\Omega$  with  $\gamma = 0.1g$  and discusses the optimal parameter range of Rabi frequency. The figure shows the optimal range of  $\Omega$  is about  $0.3g \sim 0.7g$ , which could ensure the fidelity over 0.99. Fig. 3(d) additionally considers the request to the initial state of the system. We can obtain the target state with arbitrary initial state except for the singlet state  $|\Psi^-\rangle$ .

To expound the properties peculiar to the target state, we plot the concurrence [40], classical correlation and quantum discord of the state with the full master equation in Fig. 4. It

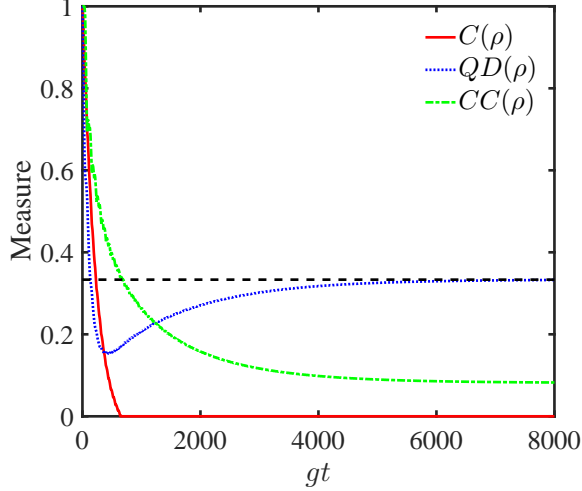


FIG. 4. The properties of the target state, which consist the concurrence (C), classical correlation (CC) and quantum discord (QD). The initial state is  $|\Psi^+\rangle$  and the black dashed line labels the number  $1/3$ .

is worth mentioning that we directly utilize the results given in Ref. [41] to measure quantum discord (QD), and the calculation of  $S(\rho_{A|B})$  is based on the positive-operator-valued measurements (POVM) locally performed on the subsystem B. The QD and the classical correlation (CC) are given as:  $QD(\rho) = \min\{Q_1, Q_2\}$ ,  $CC(\rho) = \max\{CC_1, CC_2\}$ , where  $CC_j = h[\rho_{11} + \rho_{22}] - D_j$  and  $Q_j = h[\rho_{11} + \rho_{33}] + \sum_{k=1}^4 \lambda_k \log_2 \lambda_k + D_j$ , with  $\lambda_k$  being the eigenvalues of  $\rho$  and  $h[x]$  is the binary entropy defined as  $h[x] = -x \log_2 x - (1-x) \log_2 (1-x)$ .  $D_1 = h[\tau]$ , where  $\tau = (1 + \sqrt{[1 - 2(\rho_{33} + \rho_{44})]^2 + 4(|\rho_{14}| + |\rho_{23}|)^2})/2$  and  $D_2 = -\sum_{k=1}^4 \rho_{kk} \log_2 \rho_{kk} - h[\rho_{11} + \rho_{33}]$ . Based on Fig. 4, the final state has the maximally quantum discord  $1/3$  without entanglement and the classical relation reaches the minimum. The steady state is a maximally quantum dissonant state.

Fig. 5 discusses the effect of the switching number  $N$ , where the increasing of  $N$  smooths the evolution process. It also illustrates that a high fidelity over 0.98 can be obtained with a wide range of values for  $N$ . Even if  $N = 4$  the fidelity can still get over 0.99. Thus, in actual operations, we can properly reduce the value of  $N$  to simplify the experiment.

#### IV. TWO ATOMS IN A LOSSY COUPLED-CAVITY SYSTEM

The lossy coupled-cavity system [42–46] is shown in Fig. 6. It consists of two coupled cavities which respectively trapped a four-level atom with ground states  $|0\rangle, |1\rangle$  and excited states  $|e\rangle, |r\rangle$ . The transition between  $|0\rangle$  ( $|1\rangle$ ) and  $|e\rangle$  ( $|r\rangle$ ) is coupled resonantly to the quantum field with coupling constant  $g$ , and other non-resonant transitions with detuning  $\pm\Delta$  are driven by classical field with Rabi frequencies  $\Omega_{1(2)}$  and  $\Omega'_{1(2)}$ . Thus, the Hamiltonian under the Schrödinger picture

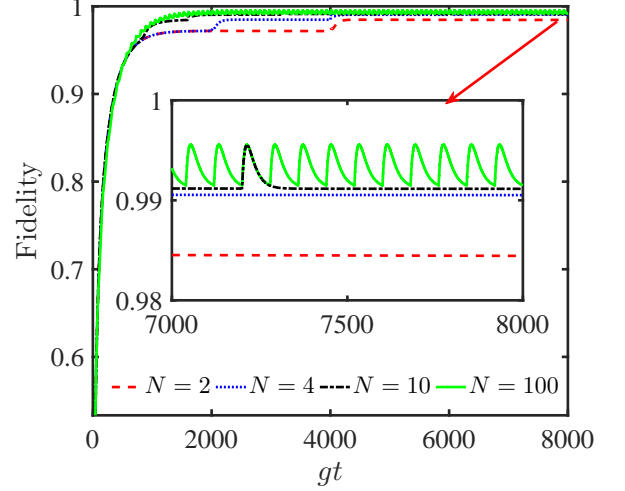


FIG. 5. Time evolution of the fidelities for the target state with different switching numbers. The inset shows the zoom-in fidelities from  $t = 7000/g$  to  $8000/g$ .

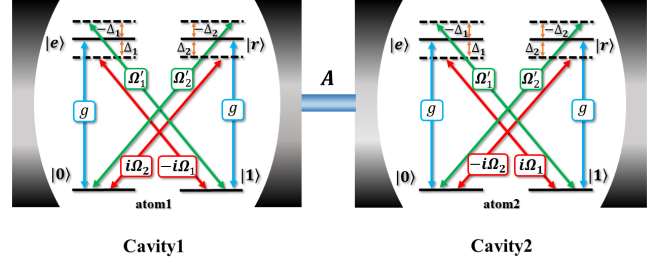


FIG. 6. Schematic view of two four-level atoms trapped in a lossy coupled-cavity array. Each atom is simultaneously driven by four classical fields with Rabi frequencies  $\Omega_{1(2)}$ ,  $\Omega'_{1(2)}$ , detuned by  $\pm\Delta_{1(2)}$  and resonantly coupled with a cavity mode. The photon can hop between two cavities with coupling strength  $A$ .

can be written as

$$\begin{aligned}
 H &= H_0 + V_s, \\
 H_0 &= \sum_{k=1}^2 \omega_0 |0\rangle_k \langle 0| + \omega_1 |1\rangle_k \langle 1| + \omega_e |e\rangle_k \langle e| \\
 &\quad + \omega_r |r\rangle_k \langle r| + \omega_c a_k^\dagger a_k, \\
 V_s &= \sum_{k=1}^2 g(|e\rangle_k \langle 0| + |r\rangle_k \langle 1|) a_k + \Omega'_1 |e\rangle_k \langle 1| e^{-i\omega'_L t} \\
 &\quad + \Omega'_2 |r\rangle_k \langle 0| e^{-i\omega'_L t} - i\Omega_1 (|e\rangle_1 \langle 1| - |e\rangle_2 \langle 1|) e^{-i\omega_L t} \\
 &\quad + i\Omega_2 (|r\rangle_1 \langle 0| - |r\rangle_2 \langle 0|) e^{-i\omega_L t} + \text{H.c.} \\
 &\quad + A(a_1^\dagger a_2 + a_2^\dagger a_1),
 \end{aligned} \tag{15}$$

where  $\omega_i$  ( $i = 0, 1, e, r$ ) are the eigenfrequencies of ground and excited states for each atom,  $\omega_c$  is the frequency of quan-

tum field,  $a_k^\dagger$  and  $a_k$  ( $k = 1, 2$ ) are creation and annihilation operators of cavity mode  $k$ ,  $\omega_L$  and  $\omega'_L$  are frequencies of classical fields. Then we switch the Hamiltonian from Schrödinger picture to the interaction picture and obtain

$$H_I = \sum_{k=1}^2 g(|e\rangle_k\langle 0| + |r\rangle_k\langle 1|)a_k + i\Omega_1 e^{i\Delta_1 t}(-1)^k |e\rangle_k\langle 1| + i\Omega_2 e^{i\Delta_2 t}(-1)^{k-1} |r\rangle_k\langle 0| + \Omega'_1 e^{-i\Delta_1 t} |e\rangle_k\langle 1| + \Omega'_2 e^{-i\Delta_2 t} |r\rangle_k\langle 0| + \text{H.c.} + A(a_1^\dagger a_2 + a_2^\dagger a_1), \quad (16)$$

where  $\Delta_1 = \omega_e - \omega_1 - \omega_L = \omega_1 + \omega'_L - \omega_e$ ,  $\Delta_2 = \omega_r - \omega_0 - \omega_L = \omega_0 + \omega'_L - \omega_r$ , and we suppose  $\Delta_1 = \Delta_2 = \Delta$ . Now we introduce a pair of delocalized bosonic modes in order to remove the localized modes as follows [46],

$$m_1 \equiv \frac{1}{\sqrt{2}}(a_1 - a_2), \quad m_2 \equiv \frac{1}{\sqrt{2}}(a_1 + a_2). \quad (17)$$

Then we have

$$H_I = \sum_{k=1}^2 \frac{g}{\sqrt{2}} m_1 e^{iAt} (-1)^{k-1} (|e\rangle_k\langle 0| + |r\rangle_k\langle 1|) + \frac{g}{\sqrt{2}} m_2 e^{-iAt} (|e\rangle_k\langle 0| + |r\rangle_k\langle 1|) + \Omega'_1 e^{-i\Delta t} |e\rangle_k\langle 1| + \Omega'_2 e^{-i\Delta t} |r\rangle_k\langle 0| + i\Omega_1 e^{i\Delta t} (-1)^k |e\rangle_k\langle 1| + i\Omega_2 e^{i\Delta t} (-1)^{k-1} |r\rangle_k\langle 0| + \text{H.c.} \quad (18)$$

We set  $A = \Delta$  to guarantee the two-photon process resonance, and choose  $\Omega_{1(2)} = \Omega'_{1(2)} = \Omega$ . Under the large detuning condition, i.e.  $|\Delta| \gg \{\Omega, g\}$ , and neglecting the Stark-shift terms, the effective Hamiltonian reads

$$H_{\text{eff}} = \sum_{k=1}^2 \frac{g\Omega}{\sqrt{2}\Delta} m_1 (-i|0\rangle_k\langle 1| + i|1\rangle_k\langle 0|) + \frac{g\Omega}{\sqrt{2}\Delta} m_2 (|0\rangle_k\langle 1| + |1\rangle_k\langle 0|) + \text{H.c.} \quad (19)$$

Based on the definition of collective spin operators  $S_x = (\sigma_{1x} + \sigma_{2x})$ ,  $S_y = (\sigma_{1y} + \sigma_{2y})$ , the effective Hamiltonian can be rewritten as

$$H_{\text{eff}} = Gm_1 S_y + Gm_2 S_x + \text{H.c.}, \quad (20)$$

where  $G = g\Omega/\sqrt{2}\Delta$ . It can be seen that the current system only involves couplings between ground states and delocalized cavity modes. Therefore, the dissipative dynamics of system can be considered as governed by the following master equation

$$\dot{\rho} = i[\rho, H_{\text{eff}}] + \sum_{k=1}^2 \frac{\kappa}{2} (2m_k \rho m_k^\dagger - m_k^\dagger m_k \rho - \rho m_k^\dagger m_k). \quad (21)$$

In the limit  $\kappa \gg |G|$ , we can adiabatically eliminating the delocalized cavity modes, and obtain the effective master equation,

$$\dot{\rho} = \mathcal{L}_{\gamma_x}(S_x)\rho + \mathcal{L}_{\gamma_y}(S_y)\rho. \quad (22)$$

Compared with the previous model, the coupled-cavity system provides the mean to realize  $\mathcal{L}_{\gamma_x}(S_x)$  and  $\mathcal{L}_{\gamma_y}(S_y)$  simultaneously. Thus the target state  $\rho = 1/3(|\Psi^+\rangle\langle\Psi^+| + |00\rangle\langle 00| + |11\rangle\langle 11|)$  can be generated using the driven-dissipative dynamics.

To verify the effectiveness of our scheme in generating MDMS, we respectively plot the populations and the fidelity of the target state with the initial state  $|00\rangle|00\rangle_c$  under the full and effective Hamiltonian in Fig. 7. We can find that these two lines perfectly coincide with each other and the state prepared by our scheme can maintain high fidelity after reaching steady state as 0.9986 in the case of steady state after about  $13000/g$ . The selections of numerical simulation parameters are  $\kappa = 0.1g$ ,  $\Omega = 0.2g$ , and  $\Delta = 100g$ .

Then we make the same discussions as Fig. 3 in the coupled-cavity system. The results are shown in Fig. 8, which show the similar behaviors of  $\kappa$ ,  $\rho_0$ ,  $\gamma$  and  $\Omega$ . Compared with the first scenario, the fidelity is higher and the final population is stable after a longer evolution time.

## V. DISCUSSION

Now, we discuss about the basic elements that maybe candidate for the intended experiment. The possible realizations of these physical models could be set up in  $^{87}\text{Rb}$  using the clock states  $|F = 1, m_F = 0\rangle$  and  $|F = 2, m_F = 0\rangle$  in the  $5S_{1/2}$  ground-state manifold as two-lower levels  $|0\rangle$  and  $|1\rangle$ . While in addition, the states to the  $|F = 1, m_F = +1\rangle$ , and  $|F = 2, m_F = +1\rangle$  of the  $5P_{1/2}$  manifold as two-higher levels  $|e\rangle$  and  $|r\rangle$  [30]. Moreover, in the first scheme, to construct the model we need the condition  $\Omega_1/\Delta_1 = \Omega_2/\Delta_2$ , which can be realized by adjusting the value of  $\Delta_{1,2}$  and  $\Omega_{1,2}$ . Identically, the second scheme needs similar conditions  $\Omega_1/\Delta_1 = \Omega_2/\Delta_2$  and  $\Omega'_1/\Delta_1 = \Omega'_2/\Delta_2$  to construct the model.

According to past works [47–50], the transition between the atomic ground level  $5S_{1/2}$  and the optical level  $5P_{1/2}$  of  $^{87}\text{Rb}$  atom is coupled to the quantized cavity mode with strength  $g = 2\pi \times 14.4$  MHz. The decay rates from higher levels to lower ones and the cavity mode are  $\gamma = 2\pi \times 3$  MHz and  $\kappa = 2\pi \times 0.66$  MHz, respectively. The Rabi frequencies  $\Omega_{1,2}$  can be tuned continuously and for the first scheme we adopt parameters  $\Omega_{1,2} = 0.3g$ ,  $\Delta_{1,2} = 76g$ ,  $N = 200$ , the fidelity of the target state is 99.41%. For the second one, we set  $\Omega_{1,2} = \Omega'_{1,2} = 0.1g$ ,  $\Delta_{1,2} = 50g$  and the fidelity is 99.56%.

In addition, Ref. [51] reported the projected limits for a Fabry–Perot cavity, which the coupling coefficient  $g = 2\pi \times 770$  MHz. Based on the corresponding critical photon number and critical atom number, we obtain  $(\kappa, \gamma) = 2\pi \times (21.7, 2.6)$  MHz. The fidelity  $F$  reaches 99.10% for the first scheme with the other relevant parameters are selected as  $\Omega_{1,2} = 0.2g$ ,  $\Delta_{1,2} = 72g$ ,  $N = 200$ . And for the second one, the fidelity is 99.67%, while other parameters are  $\Omega_{1,2} = \Omega'_{1,2} = 0.12g$ ,  $\Delta_{1,2} = 50g$ . Moreover, in a microscopic optical resonator [52], the parameters of an atom interacting with an evanescent field are  $(g, \kappa, \gamma) = 2\pi \times (70, 5, 1)$  MHz, which correspond to the fidelity  $F = 99.18\%$  with parameters

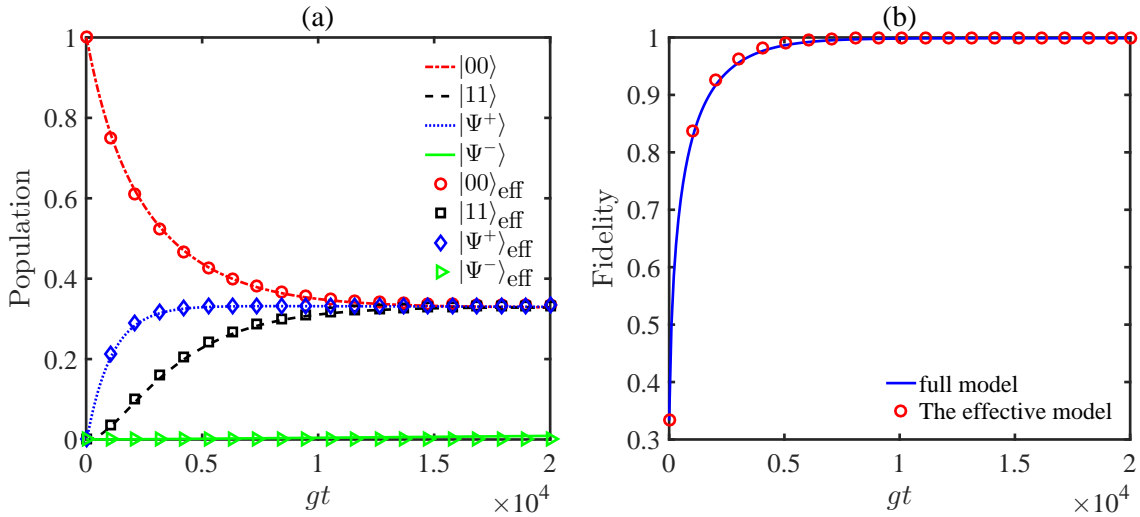


FIG. 7. Time evolution of populations (a) and fidelities (b) of the target state under the full and effective master equations, where  $\kappa = 0.1g$ ,  $\Omega = 0.2g$ ,  $\Delta = 100g$ , and  $\gamma = 0$ .

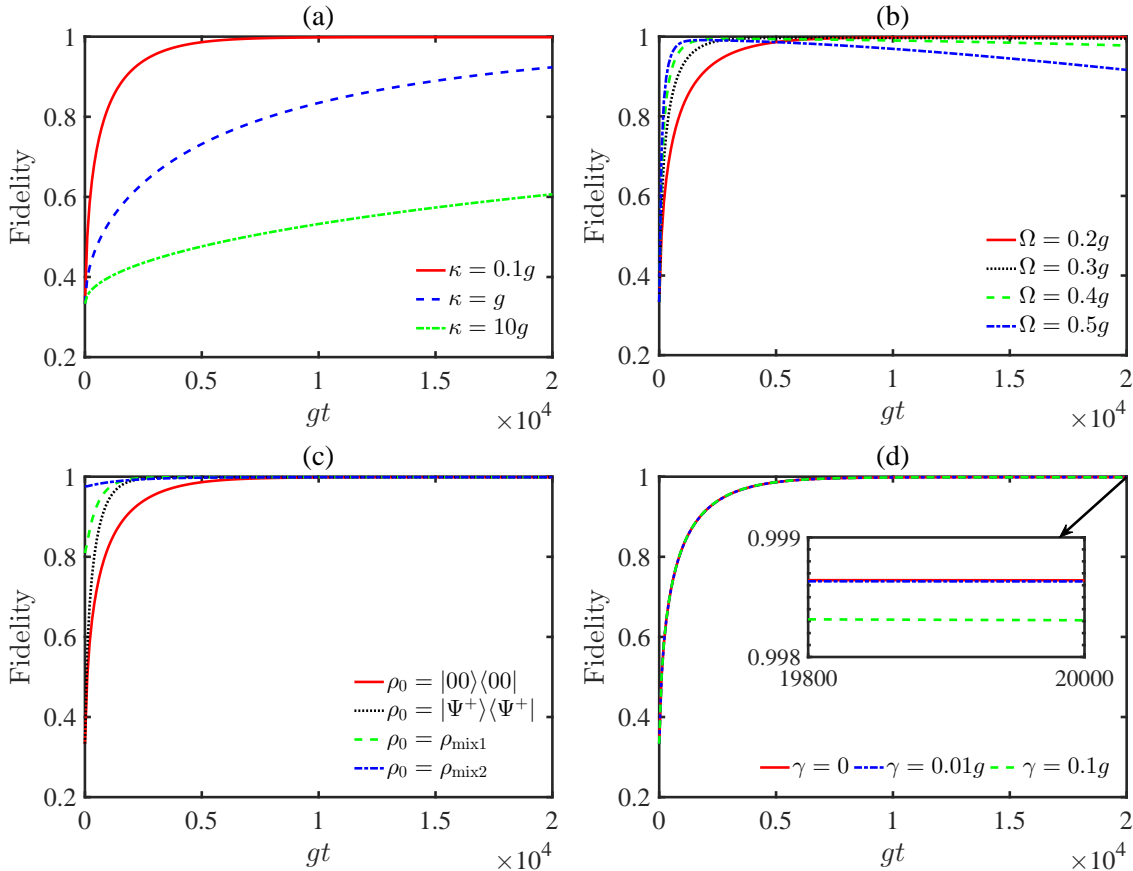


FIG. 8. Time evolutions of the target state fidelities under the full master equation with different parameters. (a) Different curves correspond to different cavity decay rates  $\kappa$ . The other parameters are  $g = 1$ ,  $\Delta = 100g$ , and  $\Omega = 0.2g$ . (b) The effect of Rabi frequencies  $\Omega$  on the target state with  $\kappa = 0.1g$  and the other parameters are same as (a). (c) Analyse different evolution processes under different initial states, where  $|\Psi^+\rangle = 1/\sqrt{2}(|01\rangle|00\rangle_c + |10\rangle|00\rangle_c)$ ,  $\rho_{\text{mix1}} = (0.1|00\rangle\langle 00| + 0.1|11\rangle\langle 11| + 0.8|\Psi^+\rangle\langle\Psi^+|) \otimes |00\rangle_c\langle 00|$ , and  $\rho_{\text{mix2}} = (0.2|00\rangle\langle 00| + 0.5|11\rangle\langle 11| + 0.3|\Psi^+\rangle\langle\Psi^+|) \otimes |00\rangle_c\langle 00|$ . (d) Discussion of the atom spontaneous emission rates  $\gamma = (0, 0.01, 0.1)g$ . The other parameters are same as above. The inset picture is the enlarge view of the part indicated by the arrow.

$\Omega_{1,2} = 0.3g$ ,  $\Delta_{1,2} = 43g$ ,  $N = 200$  in the first scheme and  $F = 99.34\%$  with parameters  $\Omega_{1,2} = \Omega'_{1,2} = 0.1g$ ,  $\Delta_{1,2} = 50g$  in the second scheme.

## VI. SUMMARY

In summary, our work provides two schemes to dissipatively produce the maximal discordant mixed state where the environment becomes a resource for states generation and breaks the time limit of the unitary dynamics. In the first scheme, by alternatively changing the phase of Rabi frequencies, the target state turns into the unique steady state of the whole process while the second one leaves out the alternating

evolutionary process by introducing a lossy coupled-cavity system. We make a comparison between two schemes. Both of them have advantages and disadvantages. For the first one, it takes shorter time to achieve the target state with the fidelity oscillated around a certain value. For the second one, although it takes longer to achieve the target state, the fidelity is stability and higher. Meanwhile, both systems have favorable resistance to the spontaneous emission of atoms, and the target state can be obtained with arbitrary initial state except for the singlet state  $|\Psi^-\rangle$ . We also discuss the relevant parameters under current experimental data and obtain high fidelities over 0.99. We hope the work may be useful for the experimental realization on quantum correlation in the near future.

- 
- [1] E. Knill and R. Laflamme, “Power of one bit of quantum information,” *Phys. Rev. Lett.* **81**, 5672–5675 (1998).
- [2] Artur K. Ekert, “Quantum cryptography based on bell’s theorem,” *Phys. Rev. Lett.* **67**, 661–663 (1991).
- [3] Charles H. Bennett and Stephen J. Wiesner, “Communication via one- and two-particle operators on einstein-podolsky-rosen states,” *Phys. Rev. Lett.* **69**, 2881–2884 (1992).
- [4] Charles H. Bennett, Gilles Brassard, Claude Crépeau, Richard Jozsa, Asher Peres, and William K. Wootters, “Teleporting an unknown quantum state via dual classical and einstein-podolsky-rosen channels,” *Phys. Rev. Lett.* **70**, 1895–1899 (1993).
- [5] P. Walther, K. J. Resch, T. Rudolph, E. Schenck, H. Weinfurter, V. Vedral, M. Aspelmeyer, and A. Zeilinger, “Experimental one-way quantum computing,” *Nature* **434**, 169– (2005).
- [6] Reinhard F. Werner, “Quantum states with einstein-podolsky-rosen correlations admitting a hidden-variable model,” *Phys. Rev. A* **40**, 4277–4281 (1989).
- [7] David W. Lyons, Abigail M. Skelton, and Scott N. Walck, “Werner state structure and entanglement classification,” *Adv. Math. Phys.* **2012**, 463610.
- [8] Harold Ollivier and Wojciech H. Zurek, “Quantum discord: A measure of the quantumness of correlations,” *Phys. Rev. Lett.* **88**, 017901 (2001).
- [9] Kavan Modi, Aharon Brodutch, Hugo Cable, Tomasz Paterek, and Vlatko Vedral, “The classical-quantum boundary for correlations: Discord and related measures,” *Rev. Mod. Phys.* **84**, 1655–1707 (2012).
- [10] Jiwon Yune, Kang-Hee Hong, Hyang-Tag Lim, Jong-Chan Lee, Osung Kwon, Sang-Wook Han, Yong-Su Kim, Sung Moon, and Yoon-Ho Kim, “Quantum discord protection from amplitude damping decoherence,” *Opt. Express* **23**, 26012–26022 (2015).
- [11] Mile Gu, Helen M. Chrzanowski, Syed M. Assad, Thomas Symul, Kavan Modi, Timothy C. Ralph, Vlatko Vedral, and Ping Koy Lam, “Observing the operational significance of discord consumption,” *Nat. Phys.* **8**, 671–675 (2012).
- [12] Fernando Galve, Gian Luca Giorgi, and Roberta Zambrini, “Maximally discordant mixed states of two qubits,” *Phys. Rev. A* **83**, 012102 (2011).
- [13] C. E. López, F. Albarrn-Arriagada, S. Allende, and J. C. Retamal, “Generation of maximally correlated states of  $(d \otimes d)$ -dimensional systems in the absence of entanglement,” *Europhys. Lett.* **120**, 10003 (2017).
- [14] M. B. Plenio, S. F. Huelga, A. Beige, and P. L. Knight, “Cavity-loss-induced generation of entangled atoms,” *Phys. Rev. A* **59**, 2468–2475 (1999).
- [15] M. B. Plenio and S. F. Huelga, “Entangled light from white noise,” *Phys. Rev. Lett.* **88**, 197901 (2002).
- [16] Giovanni Vacanti and Almut Beige, “Cooling atoms into entangled states,” *New. J. Phys.* **11**, 083008 (2009).
- [17] M. J. Kastoryano, F. Reiter, and A. S. Sørensen, “Dissipative preparation of entanglement in optical cavities,” *Phys. Rev. Lett.* **106**, 090502 (2011).
- [18] Y. Lin, J. P. Gaebler, F. Reiter, T. R. Tan, R. Bowler, A. S. Sørensen, D. Leibfried, and D. J. Wineland, “Dissipative production of a maximally entangled steady state of two quantum bits,” *Nature* **504**, 415–418 (2013).
- [19] A. W. Carr and M. Saffman, “Preparation of entangled and antiferromagnetic states by dissipative rydberg pumping,” *Phys. Rev. Lett.* **111**, 033607 (2013).
- [20] Xiao-Qiang Shao, Tai-Yu Zheng, C. H. Oh, and Shou Zhang, “Dissipative creation of three-dimensional entangled state in optical cavity via spontaneous emission,” *Phys. Rev. A* **89**, 012319 (2014).
- [21] Li-Tuo Shen, Rong-Xin Chen, Zhen-Biao Yang, Huai-Zhi Wu, and Shi-Biao Zheng, “Preparation of two-qubit steady entanglement through driving a single qubit,” *Opt. Lett.* **39**, 6046–6049 (2014).
- [22] X. Q. Shao, J. H. Wu, and X. X. Yi, “Dissipation-based entanglement via quantum zeno dynamics and rydberg antiblockade,” *Phys. Rev. A* **95**, 062339 (2017).
- [23] Xiao-Qiang Shao, “Engineering steady entanglement for trapped ions at finite temperature by dissipation,” *Phys. Rev. A* **98**, 042310 (2018).
- [24] D. X. Li and X. Q. Shao, “Unconventional rydberg pumping and applications in quantum information processing,” *Phys. Rev. A* **98**, 062338 (2018).
- [25] D. X. Li and X. Q. Shao, “Directional quantum state transfer in a dissipative rydberg-atom-cavity system,” *Phys. Rev. A* **99**, 032348 (2019).
- [26] Shi-Lei Su, Xiao-Qiang Shao, Hong-Fu Wang, and Shou Zhang, “Scheme for entanglement generation in an atom-cavity system via dissipation,” *Phys. Rev. A* **90**, 054302 (2014).
- [27] Shi-Lei Su, Qi Guo, Hong-Fu Wang, and Shou Zhang, “Simplified scheme for entanglement preparation with rydberg pumping via dissipation,” *Phys. Rev. A* **92**, 022328 (2015).



- [28] Wei Qin, Adam Miranowicz, Peng-Bo Li, Xin-You Lü, J. Q. You, and Franco Nori, “Exponentially enhanced light-matter interaction, cooperativities, and steady-state entanglement using parametric amplification,” *Phys. Rev. Lett.* **120**, 093601 (2018).
- [29] Ye-Hong Chen, Zhi-Cheng Shi, Jie Song, Yan Xia, and Shi-Biao Zheng, “Accelerated and noise-resistant generation of high-fidelity steady-state entanglement with rydberg atoms,” *Phys. Rev. A* **97**, 032328 (2018).
- [30] Emanuele G. Dalla Torre, Johannes Otterbach, Eugene Demler, Vladan Vuletic, and Mikhail D. Lukin, “Dissipative preparation of spin squeezed atomic ensembles in a steady state,” *Phys. Rev. Lett.* **110**, 120402 (2013).
- [31] Mazhar Ali, A. R. P. Rau, and G. Alber, “Quantum discord for two-qubit  $x$  states,” *Phys. Rev. A* **81**, 042105 (2010).
- [32] K.-J. Engel and R. Nagel, *One-Parameter Semigroups for Linear Evolution Equations* (Springer, New York, 2000).
- [33] M. A. Nielsen and I. L. Chuang, *Quantum computation and quantum information* (Cambridge University Press, Cambridge, 2000).
- [34] Zhi-Hua Chen, Zhihao Ma, Fu-Lin Zhang, and Jing-Ling Chen, “Super fidelity and related metrics,” *Cent. Eur. J. Phys.* **9**, 1036–1042 (2011).
- [35] V. Vedral, M. B. Plenio, M. A. Rippin, and P. L. Knight, “Quantifying entanglement,” *Phys. Rev. Lett.* **78**, 2275–2279 (1997).
- [36] V. Vedral and M. B. Plenio, “Entanglement measures and purification procedures,” *Phys. Rev. A* **57**, 1619–1633 (1998).
- [37] Robert L. Kosut, Alireza Shabani, and Daniel A. Lidar, “Robust quantum error correction via convex optimization,” *Phys. Rev. Lett.* **100**, 020502 (2008).
- [38] Paolo Giorda and Paolo Zanardi, “Quantum chaos and operator fidelity metric,” *Phys. Rev. E* **81**, 017203 (2010).
- [39] Jaroslaw Adam Miszczak, Zbigniew Puchala, Pawel Horodecki, Armin Uhlmann, and Karol Zyczkowski, “Sub- and super-fidelity as bounds for quantum fidelity,” *Quantum Inf. Comput.* **9**, 103–130 (2009).
- [40] William K. Wootters, “Entanglement of formation and concurrence,” *Quantum Inf. Comput.* **1**, 27–44 (2001).
- [41] Ferdi Altintas, Arzu Kurt, and Resul Eryigit, “Classical memoryless noise-induced maximally discordant mixed separable steady states,” *Phys. Lett. A* **377**, 53 – 59 (2012).
- [42] E. K. Irish, C. D. Ogden, and M. S. Kim, “Polaritonic characteristics of insulator and superfluid states in a coupled-cavity array,” *Phys. Rev. A* **77**, 033801 (2008).
- [43] Jaeyoon Cho, Dimitris G. Angelakis, and Sougato Bose, “Fractional quantum hall state in coupled cavities,” *Phys. Rev. Lett.* **101**, 246809 (2008).
- [44] T C H Liew and V Savona, “Multimode entanglement in coupled cavity arrays,” *New J. Phys.* **15**, 025015 (2013).
- [45] Michael Hartmann, Fernando G. S. L. Brandão, and M Plenio, “Quantum many-body phenomena in coupled cavity arrays,” *Laser Photonics Rev.* **2**, 527 – 556 (2008).
- [46] Alessio Serafini, Stefano Mancini, and Sougato Bose, “Distributed quantum computation via optical fibers,” *Phys. Rev. Lett.* **96**, 010503 (2006).
- [47] Ferdinand Brennecke, Tobias Donner, Stephan Ritter, Thomas Bourdel, Michael Khl, and Tilman Esslinger, “Cavity qed with a bose-einstein condensate,” *Nature* **450**, 268–271 (2007).
- [48] Christine Guerlin, Etienne Brion, Tilman Esslinger, and Klaus Mølmer, “Cavity quantum electrodynamics with a rydberg-blocked atomic ensemble,” *Phys. Rev. A* **82**, 053832 (2010).
- [49] Xue-Feng Zhang, Qing Sun, Yu-Chuan Wen, Wu-Ming Liu, Sebastian Eggert, and An-Chun Ji, “Rydberg polaritons in a cavity: A superradiant solid,” *Phys. Rev. Lett.* **110**, 090402 (2013).
- [50] A Grankin, E Brion, E Bimbard, R Boddeda, I Usmani, A Ourjoumtsev, and P Grangier, “Quantum statistics of light transmitted through an intracavity rydberg medium,” *New J. Phys.* **16**, 043020 (2014).
- [51] S. M. Spillane, T. J. Kippenberg, K. J. Vahala, K. W. Goh, E. Wilcut, and H. J. Kimble, “Ultrahigh- $q$  toroidal microresonators for cavity quantum electrodynamics,” *Phys. Rev. A* **71**, 013817 (2005).
- [52] Barak Dayan, A. S. Parkins, Takao Aoki, E. P. Ostby, K. J. Vahala, and H. J. Kimble, “A photon turnstile dynamically regulated by one atom,” *Science* **319**, 1062–1065 (2008).